A facile one-step strategy for development of a double network fibrous scaffold for nerve tissue engineering

2017 Biofabrication 9 025008

(http://iopscience.iop.org/1758-5090/9/2/025008)

Biofabrication

PAPER

A facile one-step strategy for development of a double network fibrous scaffold for nerve tissue engineering

RECEIVED
17 November 2016

REVISED
23 March 2017

ACCEPTED FOR PUBLICATION
24 March 2017

PUBLISHED
28 April 2017

Nasim Golafshan[1], **Hamidreza Gharibi**[2], **Mahshid Kharaziha**[1] **and Mohammadhossein Fathi**[1,3]

[1] Department of Materials Engineering, Isfahan University of Technology, Isfahan 84156-83111, Iran
[2] Department of Chemistry, Isfahan University of Technology, Isfahan 84156-83111, Iran
[3] Dental Materials Research Center, Isfahan University of Medical Sciences, Isfahan, Iran

E-mail: ma.kharaziha@gmail.com

Keywords: double network, eggshell membrane, polycaprolactone fumarate, peripheral nerve tissue engineering

Supplementary material for this article is available online

Abstract

The aim of this study was to develop a novel double network scaffold composed of polycaprolactone fumarate (PCLF) and eggshell membrane (ESM) (ESM:PCLF) by using the vacuum infiltration method. Compared to ESM, the mechanical properties of double network scaffold were significantly improved, depending on the solvents applied for double network scaffold formation; acetic acid and dichloromethane. Noticeably, the toughness and strength of double network scaffold prepared using acetic acid were significantly improved compared to ESM (26.6 and 25 times, respectively) attributed to the existence of hydrophilic functional groups in acetic acid which made ESM flexible to absorb further PCLF solution. To assess the effect of double network formation on the biological behavior of ESM, the attachment, proliferation and spreading of PC12 cells cultured on the ESM:PCLF scaffolds were evaluated. Results revealed that the number of cells attached on double network ESM:PCLF scaffold were nearly similar to ESM and significantly higher than that of on the tissue culture plate (2.6 times) and PCLF film (1.7 times). It is envisioned that the offered ESM:PCLF double network scaffold might have great potential to develop the constructs for nerve regeneration.

1. Introduction

Peripheral nerve injury is a traditional global clinical issue, which considerably affects the life quality of patients, leading to the restricted recovery (Gu *et al* 2014). The most commonly applied technique to regenerate a nerve gap consists of the nerve autograft from another site in the body. Owing to the verified difficulties of this technique consisting of deficient utilitarian recuperation and loss of capability at the donor site, nerve tissue engineering approaches were developed (Wang *et al* 2006a, Griffin *et al* 2013).

Recently, various synthetic nerve scaffolds have been developed to mimic the structure, composition and function of autographs to regenerate injured nerve tissue (Sulong *et al* 2014, Xie *et al* 2014, Golafshan *et al* 2016). These scaffolds should have critical characteristics in order to improve cell-engineered biomaterial interactions leading to stimulate the repairing and regeneration of damaged tissue. In this regard, the scaffolds are designed to structurally and mechanically simulate the complex biological structures (Koh *et al* 2008, Nectow *et al* 2012). Moreover, the engineered ideal nerve constructs should have the certain biochemical properties such as biocompatibility, ability to regenerate the nerve, semi-flexibility and easy handling during surgery (Sulong *et al* 2014). Various kinds of biomaterials have been studied for the construction of the artificial nerve scaffolds consisting of natural (such as sodium alginate (Frampton *et al* 2011), hyaluronic acid (HA) (Wang *et al* 1998) and collagen (Sulong *et al* 2014)) and synthetic (such as polycaprolactone (PCL) (Xie *et al* 2014), polyvinyl alcohol (Shokrgozar *et al* 2011), poly(lactic-*co*-glycolic acid) (PLGA) (Sulong *et al* 2014) and polycaprolactone fumarate (PCLF) (Runge *et al* 2010)) polymers. Recently, PCLF, a crosslinkable derivative of PCL, has been introduced as a promising material for the repair of segmental nerve defects (Wang *et al* 2009, Runge *et al* 2010). Compared to PCL, the mechanical, thermal, and rheological properties of PCLF could be controllable during the synthesize

process (Wang *et al* 2009). For instance, the tensile modulus of PCLF could be varied from 0.87 to 138 MPa depending on the molecular weight of the PCL precursor (Wang *et al* 2009). Moreover, cross-linkable property of PCLF makes it injectable and *in situ* harden-able to fill site defects. PCLF has also been applied in the combination with various kinds of biomaterials to develop injectable and crosslinkable scaffolds for bone and nerve tissue engineering (Jabbari *et al* 2003, Wang *et al* 2006b) as well as drug delivery vehicles (Runge *et al* 2012). Despite the successful outcomes, due to its hydrophobic nature and high stiffness, the cell-PCLF interactions are not satisfied (Wang *et al* 2009). Compared to synthetic polymers, natural polymers reveal better biocompatibility, biodegradability and non-toxicity property (Shalumon *et al* 2011). Recently, the inner chicken eggshell membrane (ESM) has been introduced as a non-toxic, biodegradable and low-cost natural material for tissue engineering applications (Ruff *et al* 2009, Lee *et al* 2010, Baláž 2014). Results demonstrated that this membrane could promote the treatment and pain relief for osteoarthritis (Ruff *et al* 2009) and over split-thickness skin graft donor sites (Yang *et al* 2003). ESM composes of a non-woven network of fibers made of biologically active compounds such as collagen, glucosamine, chondroitin and HA which are all desirable for nerve tissue engineering applications (Nakano *et al* 2003, Özgenel 2003). Due to the appropriate chemical composition and the structural properties of ESM, it might be a promising construct for nerve tissue engineering application. However, the scope of ESM applications could be restricted by its mechanical behavior. To overcome this issue, the combination of rigid/brittle networks with soft/ductile networks (double network systems) might be a noble approach (Haque *et al* 2012). Recently, double network systems has been widely applied to enhance mechanical strength and toughness of various kinds of hydrogel based materials consisting of poly (2-acrylamido-2-methyl-1-propanesulfonic acid) (PAMPS)/polyacrylamide (PAAm) (Gong 2010), gelatin/bacterial cellulose (Nakayama *et al* 2004) and poly(ethylene glycol)/poly(acrylic acid) (PEG/PAAc) (Haque *et al* 2012). Double network systems are synthesized via various techniques consisting of two-step sequential free-radical polymerization process (Gong *et al* 2003), soaking a biological gel within an aqueous monomer solution (Wang *et al* 2011), self-assembly of semi-rigid polyelectrolytes (Yang *et al* 2008) and vacuum infiltration method. Vacuum based infiltration approach is a simple and one-step technique to develop various kinds of scaffolds including polymer infiltrated into template (template synthesis) (Martín and Mijangos 2008) or vacuum infiltration of pre-sintered foams (Vogt *et al* 2010). However, this technique has not been applied for the infiltration of polymer solutions within fibrous membranes.

In this work, we employed vacuum infiltration technique in order to develop novel double network fibrous scaffolds of PCLF and ESM with controlled mechanical and biological properties for nerve tissue engineering. In this way, we also investigated the effect of solvent on the mechanical, structural, chemical and biological properties of fibrous scaffolds. It is hypothesized that the development of this flexible fibrous scaffold could simultaneously induce chemical, topographical and mechanical cues to support PC12 cell behavior.

2. Experimental section

2.1. Synthesize of PCLF prepolymer

PCLF prepolymer was synthesized according to the previously reported procedures (Wang *et al* 2006b) from PCL diol (Sigma, $M_n = 2000\ g\ mol^{-1}$). Before synthesize of PCLF, PCL diol was dried in a vacuum oven at 50 °C for 12 h. Dichloromethane (DCM, Sigma) was dried and distilled over calcium hydride (CaH_2), before the reaction. Moreover, fumaryl chloride (Sigma) was purified by distillation at 161 °C. K_2CO_3 (Sigma) was also dried at 100 °C, overnight. In order to do polycondensation approach, distilled fumaryl chloride, dried PCL diol, and dried K_2CO_3 were measured out in a molar ratio of 0.95:1:1.2. PCL diol was dissolved in DCM in the presence of K_2CO_3 (as proton scavenger). The mixture was stirred to form a slurry and fumaryl chloride dissolved in DCM was added dropwise to the slurry under a moisture-free environment in a three-necked glass flask. The reaction mixture was maintained at 50 °C under reflux for 12 h. After completing the reaction, the salts were completely removed from the mixture and the filtrate was precipitated in diethyl ether to provide a wax-like product after rotary evaporation.

2.2. Fabrication of ESM: PCLF double network fibrous scaffolds

Before fabrication of the scaffolds, commercial hens' eggs were broken and emptied. The eggshells were washed thoroughly with water. The ESM was manually separated from the shell, rinsed with distilled water to completely remove the albumen from the ESM and subsequently dried at room temperature.

ESM:PCLF scaffolds were fabricated via soaking ESM with dimension of 10 mm × 40 mm × 0.75 mm, in the PCLF solution containing bisacylphosphinoxide (BAPO, Sigma) as the photoinitiator followed by vacuum impregnation to remove air out of the ESM pores and facilitate penetration of PCLF solution into those pores. The schematic of the ESM: PCLF scaffold fabrication process is illustrated in figure 1. Primarily, homogeneous PCLF solutions consisting of various PCLF prepolymer contents (5, 10 and 15 wt%) and BAPO (5 wt% of PCLF prepolymer) were prepared and poured into a dropping funnel. In this

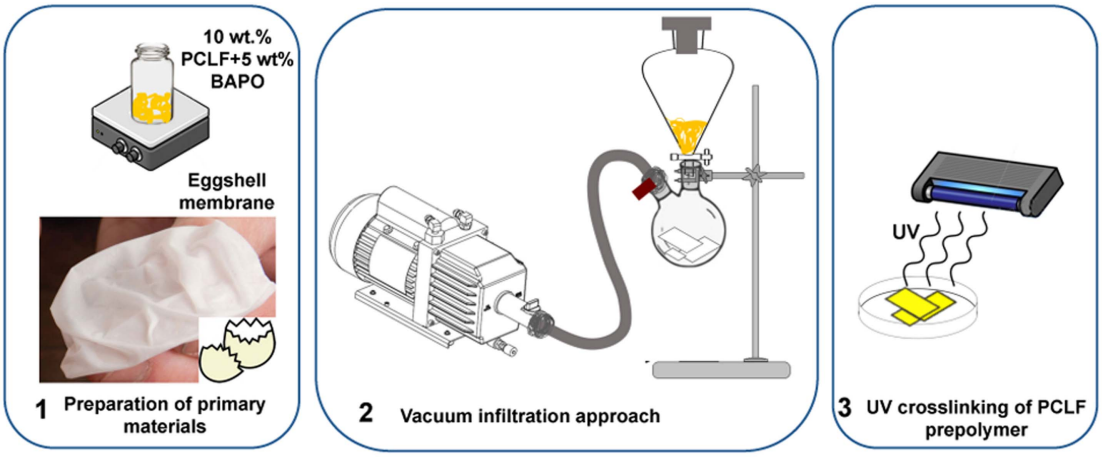

Figure 1. The schematic of the double network scaffold fabrication process consisting of three steps: (1) preparation of ESM and PCLF solution, (2) vacuum infiltration approach to entrap PCLF prepolymer solution within eggshell membrane and (3) UV crosslinking process of PCLF polymer to develop double network scaffold.

regard, two types of solvents were used to dissolve PCLF consisting of DCM and acetic acid (AA, Sigma). Separately, as-prepared and dried ESMs were put in a round-bottom flask with stopcock septum port connected to the vacuum system. After 10 min, the stopcock was opened to suck the PCLF solution over the porous ESM. After 30 min soaking of ESM in PCLF, the vacuum was stopped to allow the air pressure to force the PCLF solution into the pores of the ESM. In the next step, the flask was separated from the vacuum system and the extra PCLF was removed from the bed of the shells. Finally, ESM: PCLF scaffolds were exposed to UV light for 10 min to photo-crosslink PCLF component. According to the PCLF solvent type, the samples were named as DN-AA (solvent: AA) and DN-DCM (solvent: DCM). Moreover, in order to evaluate the scaffolds better, pure PCLF film was prepared as the comparable sample.

2.3. Characterization of ESM: PCLF double network fibrous scaffolds

The chemical composition of the prepared PCLF film and the scaffolds was characterized using a Jasco-680 Fourier Transform Infrared (FTIR) spectrophotometer (Japan) with KBr pellet. Spectra were obtained with 8 mm s^{-1} scan rate. The surface morphology of double network fibrous scaffolds was studied by scanning electron microscope (SEM, Philips, XL30) at an accelerating voltage of 10 kV, after sputter coating of the scaffolds with gold. Moreover, the average diameter of the ESM fibers ($n = 30$) was measured using the SEM images by image analysis software (Image J, National Institutes of Health, USA). The amount of encapsulated PCLF prepolymer within eggshell membrane using two different solvents (AA and DCM) (represented as the weight ratios of the ESM:PCLF) was investigated by using gravimetric method. Briefly, eggshell membranes were weighted and then impregnated in different concentrations of PCLF prepolymer (5, 10 and 15 wt%) containing BAPO followed by vacuum impregnation and UV crosslinking process as previously mentioned. Finally, the scaffolds were dried to obtain the weight of samples.

The wettability of the double network fibrous scaffolds as well as PCLF film ($n = 3$) was evaluated via water contact angle measurement with a drop shape analysis system (Sessile Drop, G10). 4 μl water droplets were applied and the contact angle between each drop and the scaffold was subsequently measured. More than five measurements on different locations of the scaffold surfaces were conducted for each type of sample and the contact angle was measured at the first seconds of falling a drop on the scaffolds. Finally, the mean value of the contact angle with the standard deviation (SD) was reported. The swelling of the double network fibrous scaffolds was investigated at room temperature by using gravimetric method. Briefly, following measurement the weight of dried scaffolds, they were swollen in deionized water. In different time points at room temperature, the scaffolds were carefully weighted after wiping off the excessive water. Finally, mass swelling ratio of the scaffolds at each specific time (t) was calculated according to the following equation (equation (1)) (Jiankang *et al* 2009):

$$\text{Mass swelling} = \frac{Wt - Wd}{Wd} \times 100, \qquad (1)$$

where W_t and W_d are the mass of the swollen and dried scaffolds, respectively.

Tensile properties of double network fibrous scaffolds as well as PCLF film were determined at ambient temperature (25 °C) and wet condition using Hounsfield H25KS tensile tester, with a load cell capacity of 10 N and rate of 3 mm min^{-1}. Specimens were cut in the rectangular shapes and dimension of 10 mm × 40 mm. Before mechanical testing, the samples were immersed in phosphate buffered saline (PBS) for one

day. The stress–strain curves ($n = 5$) were plotted and the mechanical characteristics such as tensile strength, elastic modulus and energy per volume (toughness) were calculated. While the elastic modulus was estimated from the linear region of the stress–strain curves, tensile toughness was determined from the area under the stress–strain curves after plastic deformation and ultimate tensile strength was estimated from the maximum point of each curve. Moreover, to evaluate the morphology and fiber diameter changes, before complete fracture (at 80% elongation), the samples were gold coated and finally assessed using SEM imaging.

2.4. *In vitro* cell culture

In order to evaluate the effects of double network fibrous scaffold on the cell responses, PC12 cells were cultured on the scaffolds and the cell attachment, proliferation and spreading were investigated. PC12 cells purchased from Pasteur Institute of Iran (NCBI code: C153) were cultured in Dulbecco's modified Eagle medium (DMEM-Hi, Bioidea, Iran) supplemented with 10% fetal bovine serum (Bioidea, Iran), 5% horse serum (HS, Baharafshan, Iran) and 1% streptomycin/penicillin (Bioidea, Iran). Before cell seeding, the scaffolds as well as PCLF film were sterilized via 30 min soaking in 70% ethanol, 2 h exposing to UV light and finally immersing in culture medium overnight. PC12 cells (within passages 10–12) at a density of 10^4 cells/well were seeded onto the scaffolds, PCLF film and tissue culture plate (TCP, control). Cells were incubated at 37 °C under 5% CO_2 condition for 7days and the medium was changed every 3 days.

2.4.1. MTT assay

The survival rate of PC12 cells was studied by 3-(4, 5-dimethylthiazolyl-2)-2, 5-diphenyl tetrazolium bromide (MTT) purchased from Sigma-Aldrich. At days 1, 4 and 7 of incubation, culture medium was threw away, the wells were washed with PBS and the samples as well as control ($n = 3$ per group) were incubated with MTT solution (0.5 mg ml^{-1} MTT reagent in PBS) for 4 h. The dark blue formazan crystals were solubilized with the MTT solvent (dimethyl sulfoxide (DMSO), Sigma-Aldrich) and kept for 30 min at 37 °C on a shaker. Subsequently, 100 μl of dissolved formazan solution of each sample was moved to 96-well plate and the optical density of each well was measured with a microplate reader (Bio Rad, Model 680 Instruments) against DMSO (blank) at a wavelength of 540 nm and a reference filter of 630 nm. The relative cell survival was estimated according to the following equation (equation (2)) (Golafshan *et al* 2016):

$$\text{Relative cell survival (\%)} = \frac{A_{\text{Sample}} - A_{\text{b}}}{A_{\text{control}} - A_{\text{b}}} \times 100, \quad (2)$$

where A_{sample}, A_{b} and A_{control} stand for the absorbance of sample, blank (DMSO) and TCP, respectively.

2.4.2. Cell attachment and spreading

Cell attachment on the various samples was quantified by counting cellular nuclei after a day of culture. To stain the nuclei of the cells, after rinsing with PBS, the samples were fixed in 4% paraformaldehyde (PF, Sigma) solution in PBS for 30 min. After preparation of 0.1 μg ml^{-1} of DAPI (40,6-diamidino-2-phenylindole) (Sigma) solution in PBS, it was added to each sample and kept in the incubator for 10 min to stain the nuclei. After three times rinsing with PBS, the fluorescence images of the cells' nuclei were captured from 3 to 5 different regions of the samples and the number of cell nuclei within each field was counted using NIH Image J software.

The spreading of PC12 cells cultured on the scaffolds for 7 days was evaluated by SEM technique. After 3 h fixation with 2.5 (v/v)% glutaraldehyde (Sigma), the samples were rinsed with PBS, and dehydrated in the graded concentrations of ethanol (30, 50, 70, 90, 95 and 100 (v/v)%) for 10 min each, respectively. Finally, the samples were treated via immersing in 50% alcohol-hexamethyldisilazane (HMDS, Sigma) solution (v/v) for 10 min and then in pure HMDS for 10 min. Finally, they were dried in a desiccator overnight, gold-coated and evaluated using SEM imaging.

2.5. Statistical analysis

The data in this study were analyzed using one-way ANOVA analyses and reported as mean ± SD. To determine a statistically significance difference between groups, Tukey's post-hoc test using GraphPad Prism Software (V.6) with a P-value < 0.05 was applied to be significant.

3. Results and discussion

3.1. Characterization of the ESM: PCLF double network scaffold

Despite the fantastic properties of ESM, low mechanical properties of this membrane may restrict its application for engineering the tissues exposing to the static and dynamic stresses such as nerve. In this way, in order to overcome this issue, double network formation could be a promising way. In this study, according to figure 1, vacuum infiltration technique as a simple and versatile approach was applied to develop double network fibrous scaffolds based on ESM as the soft and PCLF as the hard components. In order to investigate the effect of PCLF prepolymer concentration on the amount of loaded PCLF, various concentrations of PCLF prepolymer solution (5, 10 and 15 wt%) were applied and the weight changes of the scaffolds were estimated. The weight ratio of PCLF: ESM as the function of PCLF prepolymer concentration as well as solvent type (AA and DCM) is presented in supplementary figure S1 available at stacks.iop.org/BF/9/025008/mmedia. Our result clearly revealed that DN-AA scaffold consisted of significantly more

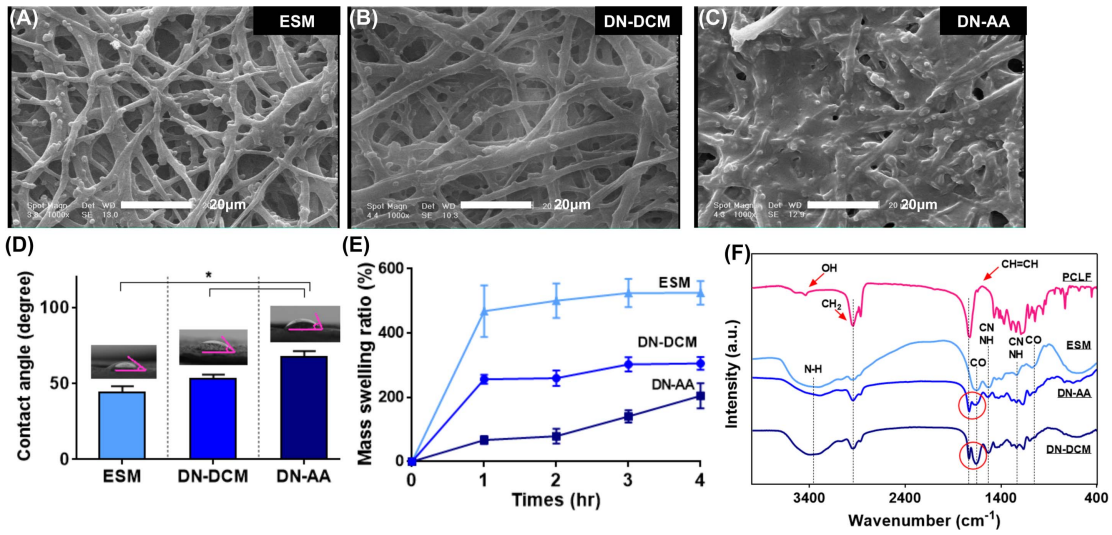

Figure 2. Structural, physical and chemical properties of double network scaffolds; SEM images of (A) ESM as well as (B) DN-DCM and (C) DN-AA scaffolds. The amount of loaded PCLF effected (D) the water contact angle and (E) swelling ratio of the scaffolds. (F) FTIR spectra of PCLF prepolymer, ESM, DN-DCM and DN-AA scaffolds as well as PCLF prepolymer.

PCLF content compared to DN-DCM scaffold. In this regard, when AA was used as solvent, the weight ratio of PCLF:ESM was about 0.83:1, 2.34:1 and 2.80:1 at PCLF prepolymer concentration of 5, 10 and 15 wt%, respectively. In another word, the weight ratio of PCLF:ESM reduced when DCM was used as solvent (0.33:1, 0.90:1 and 1.15:1 at PCLF prepolymer concentration of 5, 10 and 15 wt%, respectively). It could be due to the hydrophilic characteristic of ESM, which has more intermolecular interaction and swelling in the polar protic solvents such as AA compared to the less-polar protic solvents such as DCM confirming more PCLF prepolymer penetration within the ESM pores. Moreover, while the weight ratio of PCLF:ESM at PCLF prepolymer concentrations of 5 and 10 wt% revealed significant differences at both hybrid scaffold types (DN-AA and DN-DCM) ($p < 0.05$), increasing the concentration of PCLF prepolymer solution to 15 wt% did not significantly modulate ESM:PCLF weight ratio ($p > 0.05$). Therefore, the samples consisting of primarily 10 wt% PCLF prepolymer solution were used for the next experiments.

The representative microstructure images of the ESM as well as ESM:PCLF double network fibrous scaffolds prepared using two different solvents (DN-AA and DN-DCM) are presented in figure 2. The ESM (figure 2(A)) revealed the random fibrous morphology with almost large pores. After incorporation of PCLF polymer within the ESM matrix using the vacuum infiltration method, the fiber size of ESM enhanced and its pore size reduced, depending on the applied solvents (AA and DCM) confirming the formation of double network systems. In the case of DN-DCM (figure 2(B)), the PCLF mostly covered the fibers and enlarged the average fiber size of ESM from $1.18 \pm 0.19\,\mu$m to $1.3 \pm 0.2\,\mu$m. Moreover, the pore size of DN-DCM did not significantly change confirming that PCLF solution did not penetrate within the structure of ESM. When AA was used as solvent (figure 2(C)), PCLF polymer not only shielded the fibers but also penetrated within the large pores of ESM leading to the fusion of the ESM fibers together. In this condition, the average fiber diameter of ESM significantly ($P < 0.05$) enhanced to $1.8 \pm 0.3\,\mu$m, while the pore size noticeably reduced ($P < 0.05$) from $11.6 \pm 2.2\,\mu$m to less than $4.8 \pm 0.9\,\mu$m which may have critical role on the mechanical and biological properties of double network constructs. Owing to the presence of large amounts of polar and hydrophilic functional groups ($-$OH, $-CO_2H$, $-NH_2$, $-$CHO, $-SO_4H$, $-$SH) (Nakano *et al* 2003), ESM could have obviously more interaction and swelling in the polar protic solvents such as AA leading to more penetration of PCLF prepolymer.

The results of water contact angle measurements (figure 2(D)) and mass swelling ratio (figure 2(E)) of the scaffolds confirmed the hydrophilicity of double network-systems. However, depending on the solvent type, the swelling ratio and contact angle value were estimated different. Noticeably, the mass swelling ratio was decreased from $525.1 \pm 37.1\%$ (at ESM) to $204.7 \pm 39.1\%$ (at DN-AA) and the water contact angle enhanced from $44.1 \pm 3.3°$ (at ESM) to $67.3 \pm 3.2°$ (at DN-AA). Moreover, compared to DN-DCM scaffold, DN-AA was more hydrophobic due to the presence of PCLF in its network and hydrophobicity of PCLF backbone. Therefore, by the selection of an appropriate solvent, it is possible to control hydrophilicity and hence, degradation rate of the scaffolds.

Double network fibrous scaffolds were also characterized using FTIR spectroscopy in order to confirm the presence of crosslinked PCLF in the structures. Figure 2(F) presents the FTIR spectra of ESM and ESM:

PCLF double network fibrous scaffolds as well as PCLF prepolymer, before crosslinking. PCLF prepolymer revealed the absorption band at 1642 cm^{-1} assigned to the C=C due to the fumarylation of PCL-diol (Wang *et al* 2006b). Moreover, ESM consisted of the significant peaks at 3310 cm^{-1} (attributed to the O–H and N–H stretching mode), 3064 cm^{-1}, 2935 cm^{-1}, and 2870 cm^{-1} (corresponded to the asymmetric stretching vibrations of the C–H bonds presented in =C–H and $=CH_2$ groups), 1648 cm^{-1} (due to the C=O stretch of amides), 1525 cm^{-1} (attributed to the CN stretching/NH bending modes), and 1234 cm^{-1} (corresponded to the CN stretching/NH bending modes), which the last three peaks can be assigned to the amide I (1648 cm^{-1}), amide II (1525 cm^{-1}), and amide III (1234 cm^{-1}) vibrations of the glycoprotein mantle of the fibers, respectively (Dong *et al* 2007, Kong and Yu 2007, Colthup 2012). Incorporation of PCLF within the structure of ESM did not affect the position of the major bands of ESM. In addition, the strong bands at 1726, 1170 and 1105 cm^{-1}, which were similarly detected in the FTIR spectrum of PCLF prepolymer, were the characteristics of skeletal ester, ether stretches and vibration of C–COO– and C–O–C groups of PCLF, respectively, demonstrating the successful penetration of PCLF into the ESM construct. However, the relative absorption intensities of the major bands at 1724 cm^{-1} (attributed to the PCLF) and 1648 cm^{-1} (attributed to the ESM) at FTIR spectrum of DN-AA scaffold enhanced compared to those of DN-DCM one which confirmed more PCLF penetration within the ESM pores, in the employment of AA as the polar protic solvent. It is noteworthy to mention that the disappearance of fumarate double bond after photo-crosslinking indicated the consumption of double bonds of DN-AA and DN-DCM during photo-crosslinking process to form polymer networks into the ESM matrix (Wang *et al* 2006b).

The FTIR spectra of the ESM:PCLF scaffolds fabricated using various PCLF prepolymer concentrations (5, 10 and 15 wt%) and solvents (AA and DCM) were also evaluated to precisely study the effects of diverse PCLF prepolymer concentrations on the amounts of encapsulated PCLF (supplementary figure S2). Two main characteristic peaks of two components were the absorption band centered at 1648 cm^{-1} attributed to stretching of the C=O of amide group ($C=O_{amide}$) in ESM and the sharp band at 1724 cm^{-1} corresponded to stretching of the C=O group of ester ($C=O_{ester}$) in PCLF. Increasing PCLF prepolymer concentration from 5 to 15 wt% resulted in an increase in the absorbance of the $C=O_{ester}$ peak at 1724 cm^{-1} and the gradually weakening of the relative intensity of $C=O_{amide}$ over $C=O_{ester}$ confirming more penetration of PCLF prepolymer in the ESM matrix. Moreover, figure S2 reveals the relationship between PCLF:ESM ratio as proportional to the ratio of A_{ester} ($C=O_{ester}$ in PCLF) to A_{amide} ($C=O_{amide}$ in ESM) and the concentration of PCLF. Compared to the samples prepared using AA solvent, application of DCM resulted in reduced C=O stretching vibration of ester peak ($\nu = 1724\ cm^{-1}$). For instant, the intensity ratio of A_{ester}/A_{amide} revealing the more penetration PCLF prepolymer in the ESM matrix was 1.05, 1.25, and 2.15 in DN-AA (figure S2(A)) and 0.51, 0.77, and 1.63 for DN-DCM (figure S2(B)) for various PCLF prepolymer concentrations (5, 10 and 15 wt%, respectively).

The double network fibrous scaffolds were further characterized using mechanical evaluation of the scaffolds. The typical stress–strain curves of double network scaffolds after UV crosslinking treatment and soaking in PBS for 1 h are shown in figure 3(A). While the PCLF film failed after bearing low strain (78 ± 6%), the ESM and double network scaffolds revealed 1.4 times more elongation. Furthermore, there was not a meaningful difference between the elongation of ESM and double network scaffolds. However, there was a significant difference between the mechanical strength of the double network fibrous scaffolds made by AA (DN-AA) and DCM (DN-DCM). These trends indicated that the mechanical properties of the various scaffolds were strictly controlled by the amounts of penetrated PCLF within the ESM matrix. In this regards, DN-AA scaffold revealed robust construct with considerably higher tensile strength due to the further amounts of entrapped PCLF and the encounter between PCLF and fibers. However, in the case of DN-DCM, due to the less amount of PCLF content, the mechanical strength of the scaffold was near to the ESM and lower than that of PCLF.

Tensile test was also applied in order to estimate the elastic modulus (figure 3(B)), tensile toughness (figure 3(C)) and ultimate tensile strength (figure 3(D)) of the ESM, double network fibrous scaffolds and PCLF film from stress–strain curves according to the ASTM D882. The main issue of PCLF film, used as nerve graft, is its high elastic modulus preventing from bending without tearing (Wang *et al* 2009). According to figure 3(B), the development of double network systems of PCLF and ESM resulted in the noticeably reduction in elastic modulus of the scaffolds compared to PCLF ($P < 0.05$). For instance, by using AA as the solvent, the elastic modulus of the double network-systems was noticeably declined from 28.2 ± 6.1 MPa (for PCLF) to 18.4 ± 1.0 MPa (DN-AA), respectively ($P < 0.05$). In addition, tensile toughness is the essential characteristic of the neural engineering scaffolds allowing them to recover once a construct is employed around the nerve (Tian *et al* 2015), to manipulate easily, to bear shocks and vibrations, to cut into strips or other shapes and to be rolled up into 3D tubular construct (Davis *et al* 1987, Yucel *et al* 2010). Compared to ESM, the toughness of DN-AA and DN-DCM fibrous scaffolds improved from 0.4 ± 0.4 MPa to 10.6 ± 1.0 MPa and 1.0 ± 0.2 MPa, respectively (figure 3(C)). Moreover, compared to ESM, the tensile strength of the DN-AA (figure 3(D)) remarkably enhanced (around 25 times), while in the case of DN-DCM, it was not

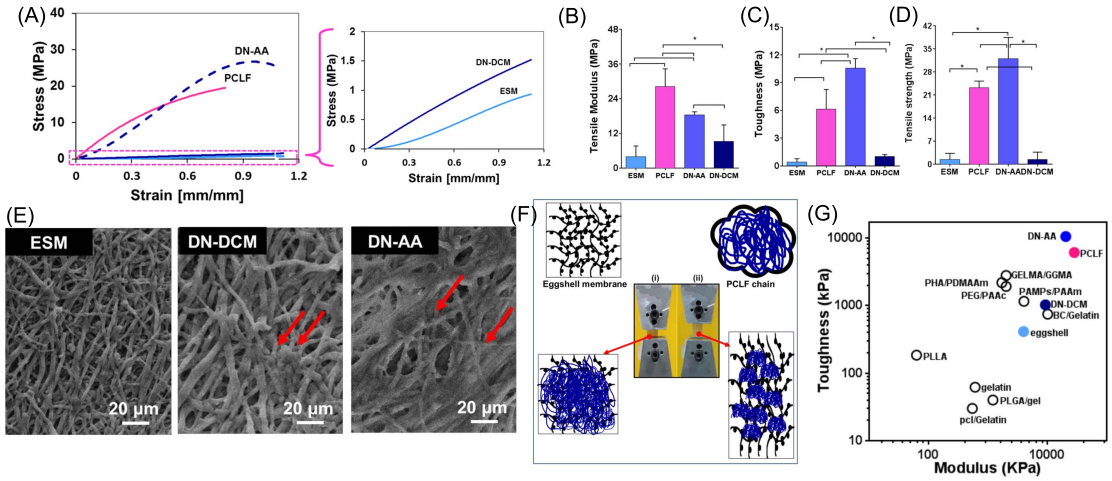

Figure 3. Mechanical properties of double network scaffolds; (A) representative tensile stress–strain plots for the ESM, PCLF polymer as well as DN-DCM and DN-AA scaffolds after 1 h immersing in PBS. Comparison of (B) the tensile modulus, (C) the tensile toughness and (D) tensile strength of scaffolds ($^{*}P < 0.05$). (E) SEM images of various scaffolds, under uniaxial tensile loading, before complete fracture (at 80% elongation). (F) A schematic illustrating the double network scaffolds of PCLF as brittle and eggshell membrane as soft network, (i) before and (ii) after tensile loading. In the double network fibrous scaffolds, PCLF assisted the filling of the crack-like defects preventing crack propagation in the ESM surface by energy dissipating mechanism. (G) A comparison of the elastic modulus and toughness for previously reported double network systems (open circle) and the offered double network scaffolds (Gong et al 2003, Yang et al 2008, Zhang et al 2009, Prabhakaran et al 2011, Shin et al 2012a).

considerable ($P > 0.05$). Furthermore, compared to DN-DCM, the mechanical properties of DN-AA noticeably enhanced. For instance, the tensile toughness of the DN-AA was about 10 times greater than that of DN-DCM confirming the role of PCLF content as well as pore and fiber sizes of the scaffolds on their mechanical properties. According to figures S1 and S2 as well as SEM images of the scaffolds at figure 2, incorporation of more PCLF within ESM matrix at DN-AA, due to the greater relative polarity of AA compared to DCM, resulted in reduced pore size and increased fiber size which improved the resistance of the porous scaffolds against mechanical load. The effects of incorporated PCLF during mechanical test of double network scaffolds were studied using SEM images presented in figure 3(E). According to SEM images, during the tensile test, most of the fibers elongated in the direction of loading. Moreover, the average fiber sizes of all scaffolds reduced. For example, the average fiber diameter of ESM ($1.18 \pm 0.19\ \mu$m) reduced to $0.8 \pm 0.31\ \mu$m ($p < 0.05$). Furthermore, similar to the fiber diameter of samples before loading, the average fiber size of double network scaffolds (DN-DCM and DN-AA) was greater than that of pure ESM ($1.8 \pm 0.3\ \mu$m and $1.3 \pm 0.5\ \mu$m, respectively) suggesting that the surface of fibers was covered using PCLF. However, compared to the pure ESM and DN-DCM, the pore size of DN-AA scaffold was mostly occupied using PCLF network fragments. According to the mechanical properties, it could be concluded that when the external load was applied on the double network scaffolds, specifically DN-AA consisting of greater amount of PCLF, the PCLF network fragments perforated into the gaps of ESM acted as a crosslinker of ESM fibers and sacrificial bonds which partially ruptured to dissipate energies leading to the considerable improvement of the mechanical strength. This behavior was explained in the schematic presented in figure 3(F). The incorporation of PCLF solution into the ESM resulted in the filling of the large pores of matrix due to the applied vacuum infiltration of PCLF. In this condition, PCLF probably assisted the filling of the crack-like defects preventing crack propagation in the ESM surface by energy dissipating mechanism. Surprisingly, by employment of AA solvent, due to its more hydrophilicity nature than DCM, most of the pores were filled with PCLF solution. In this condition, during tensile test, the PCLF network portions entered into the small pores of ESM could dissipate energy resulted in the substantial enhancement of the mechanical properties. In another research, Nakayama *et al* (2004) synthesized a double network gel consisting of bacterial cellulose and gelatin. They revealed that the fracture strength and elastic modulus of double network gel under elongation stress were about 3.8 MPa and 21 MPa, respectively, which were significantly higher than those of mother hydrogels (2.2 MPa and 2.9 MPa for bacterial cellulose and 0.2 MPa and 1.8 MPa for gelatin, respectively). Shin *et al* (2012a) also investigated the double network hydrogel of gellan gum methacrylate (GGMA), the rigid and brittle first network, and gelatin methacrylamide (GelMA), the soft and ductile second network. They revealed that double network hydrogel exhibited higher failure stress (6.9 MPa) than single network (SN) hydrogel (0.6 MPa) due to an increase in the equilibrium polymer concentration and the double network structure. From the above experimental findings and the fact that the ESM are quite soft and weak against tensile force, double network fibrous scaffold with adequate amount of PCLF component revealed significantly

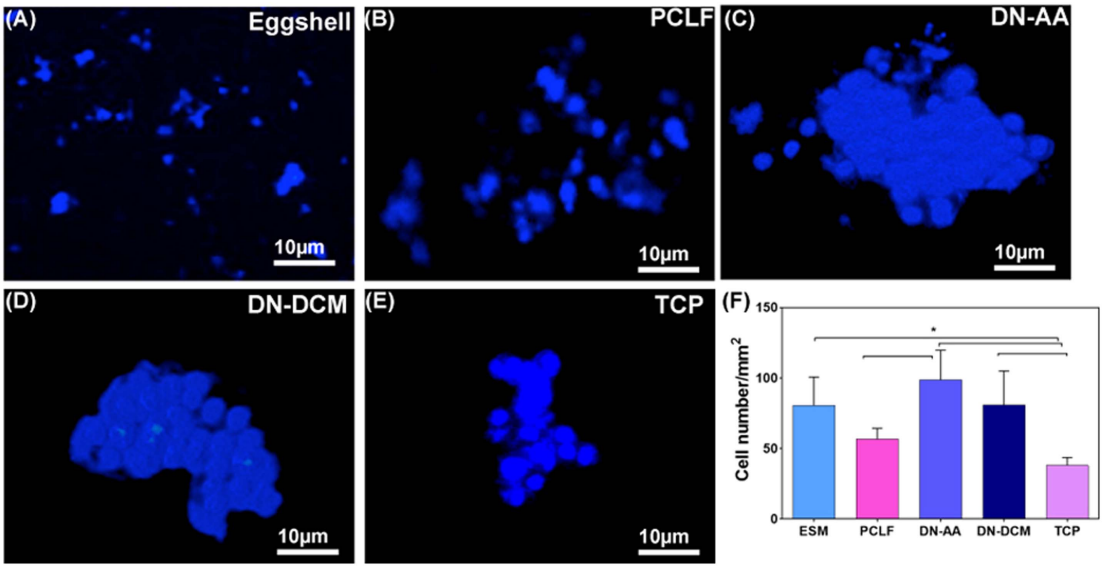

Figure 4. PC12 cell attachment on the double network scaffolds; representative fluorescent images of DAPI-stained PC12 cells cultured for 1 day on (A) ESM, (B) PCLF film, (C) DN-AA scaffold and (D) DN-DCM scaffold as well as (E) tissue culture plate (TCP) as control. (F) The quantified cell numbers attached on the surface of various samples ($^{*}P < 0.05$).

more strength and toughness than ESM matrix and less stiffness than PCLF which could be better pinch to use as nerve graft.

Our results presented that DN-AA fibrous scaffold revealed superior toughness against elastic modulus as compared to the previously reported scaffolds which made it suitable for nerve tissue engineering (figure 3(G)) (Gong *et al* 2003, Yang *et al* 2008, Zhang *et al* 2009, Prabhakaran *et al* 2011, Shin *et al* 2012a). For instance, while the toughness of DN-AA scaffolds was about 10.6 ± 1.0 MPa, GelMA-GGMA scaffold showed the toughness of about 2.8 MPa. Furthermore, our results revealed that, the toughness, elastic modulus and strength of DN-AA scaffold were the nearest to those of the nerve tissue (strength and elastic modulus of nerve were are about 12 and 7 MPa, respectively) (Golafshan *et al* 2016).

3.2. Cellular responses to the ESM: PCLF double network scaffold

To assess the utility of ESM:PCLF double network fibrous scaffolds for nerve tissue engineering, we seeded ESM, PCLF film and TCP with PC12 cells and investigated the effects of architecture and mechanical properties of the samples on the cell behavior. For the primary evaluation of the cell interaction with samples, cell attachment was estimated by counting DAPI-stained nuclei after one day of culture (figure 4). The average cell number was estimated using at least five images captured at numerous areas of the samples (figure 4(F)). Results confirmed that cell attachment on the ESM and double network scaffolds was drastically superior compared to TCP and PCLF film ($P < 0.05$). For instance, 2.6-fold and 1.7-fold further PC12 cells attached on the DN-AA (98.8 ± 19.0 cells) than on TCP (38.0 ± 4.9 cells) and PCLF film (56.7 ± 6.2 cells), respectively ($P < 0.05$). However, the differences of cell number attached on the different double networks and ESM were statistically negligible ($P > 0.05$). Moreover, the cell numbers attached on the DN-AA was slightly greater than on the DN-DCM scaffold. It is well known that cell attachment is stronger on stiff substrates compared to the compliant (soft) ones (Discher *et al* 2005). Therefore, higher cell attachment on the double network scaffolds and ESM compared to PCLF film is expected to be mainly dominated by their fibrous architecture and higher surface-to-volume ratio as well as their improved hydrophilicity which eventually enriched protein adsorption as well as selective protein secretions providing a favorable substrate for cell attachment (Woo *et al* 2003). However, greater cell attachment of DN-AA scaffold than DN-DCM might be due to higher mechanical properties of this scaffold. Consistent with our findings, previous studies also confirmed higher cellular attachment on the scaffolds with higher mechanical properties (Shin *et al* 2012b, Kharaziha *et al* 2013, Kharaziha *et al* 2014).

The metabolic activity of the proliferating cells was also evaluated after 1, 4 and 7 days of culture on the different double network scaffolds, ESM and PCLF film compared to control by MTT assay (figure 5). Overall, the proliferation of PC12 cells seeded on the various samples gradually enhanced from day 1 up to day 7. Specifically, the proliferation of cells cultured on DN-AA scaffolds statistically improved from 85.3 ± 12.1%(control) (at day 1) to 362.6 ± 10.1% (control) (at day 7) ($P < 0.05$). Moreover, after 7 days of culture, the proliferation of PC12 cells cultured on ESM based scaffolds was considerably higher than that of on the PCLF film. For instance, the cell proliferation on the DN-AA fibrous scaffold was found to be 2.6

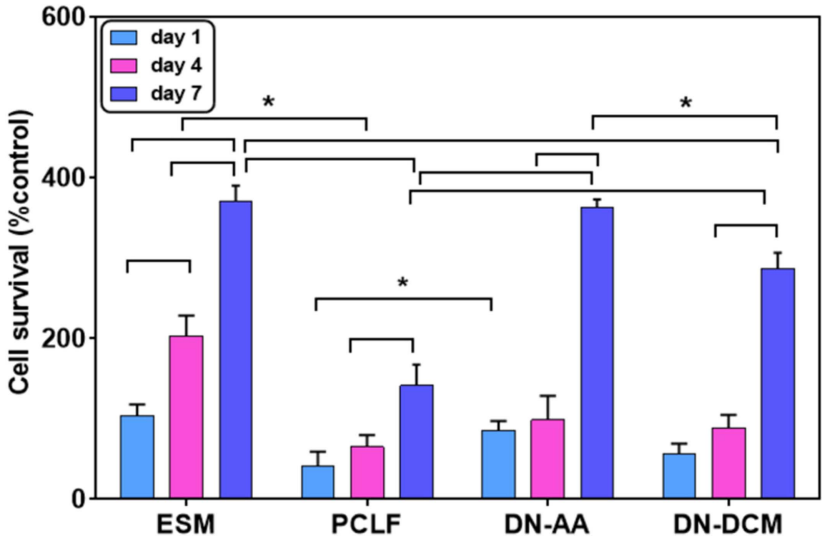

Figure 5. Cell survival of PC12 seeded on the various samples measured using MTT assays after 1, 4 and 7 days of culture. The absorbance was normalized against the control (TCP) at each time interval ($^{*}P < 0.05$).

times greater than that of on the PCLF film. Moreover, the cell proliferation on the ESM (370.56 ± 19.61% (control)) was not noticeably different from that on the DN-AA scaffold. In addition, enhanced PCLF encapsulation within ESM scaffold (DN-AA versus DN-DCM) promoted proliferation of the PC12 cells suggesting that PC12 metabolic activity was a function of mechanical properties of the scaffolds. This result was similarly reported, previously (Shin *et al* 2012b, Kharaziha *et al* 2013, Kharaziha *et al* 2014, Kim *et al* 2016). Our results revealed that the incorporation of PCLF as the second component in the eggshell matrix could noticeably enhance its mechanical properties while would not reduce the cell metabolic activity. These desirable properties could make this scaffold a suitable candidate for engineering of nerve and other soft tissues.

The morphology of PC12 cells cultured for 7 days on the various scaffolds as well as PCLF film was studied using SEM imaging (figure 6). While PC12 cells seeded on the PCLF film preserved a rounded morphology, relatively spread cells could be observed on the various eggshell based scaffolds. High magnification images could clearly show the speeding of the cells not only on the surface but also within the depth of scaffold which could be due to the large pore size of the scaffolds and appropriate surface properties. Specifically, cells with polygonal appearance could be observed on the surface and within the depth of DN-AA scaffold due to large pores and the hydrophilicity of the scaffolds. PC12 cells connected to the neighboring cells, implying their preparedness and initiation to differentiate (Tian *et al* 2015).

Our results suggested that PC12 cell attachment, proliferation and spreading depended on the mechanical, chemical and structural (fibrous versus film) characteristics of the substrates. In this regard, it could be accomplished that greater cell attachment on the ESM than TCP and PCLF film might be due to its further hydrophilicity (due its chemical composition) as well as its fibrous structure. The inner layer of eggshell is a unique fibrous construct mainly composed of collagen (35%) and hyaluronic acid (5%–10%) (Sah and Rath 2016). These two polymers have been widely employed to develop hydrogel based constructs for nerve regeneration (Kitahara *et al* 1998, Wang *et al* 1998). Therefore, the chemical composition of ESM as well as large surface area-to-volume ratio of this fibrous construct could promote the intercellular signaling leading to the enhanced cellular proliferation. In another word, according to figure 3(A), the weak mechanical properties of ESM could limit its applications for various tissue engineering applications. Our result demonstrated that by the fabrication of double network fibrous system based on ESM (soft section) and PCLF (hard section), it is possible to control the mechanical properties of ESM while preserve the biological properties.

Based on our results, the suggested double network fibrous scaffolds developed using vacuum infiltration method presented an exciting option to be applied in the engineering of various tissues, due to the adjustable mechanical and physical properties via easy and rapid modification processes. Moreover, the mechanical and electrical properties of the double network could also be modulated via the incorporation of various kinds of nanoparticles in the PCLF component during the vacuum process making them appropriate for various soft and hard tissues. Moreover, the encapsulation of various drugs and bioactive molecules during the formation of PCLF (second network) could enhance cell function and therefore tissue regeneration. Overall, this double network system was built on

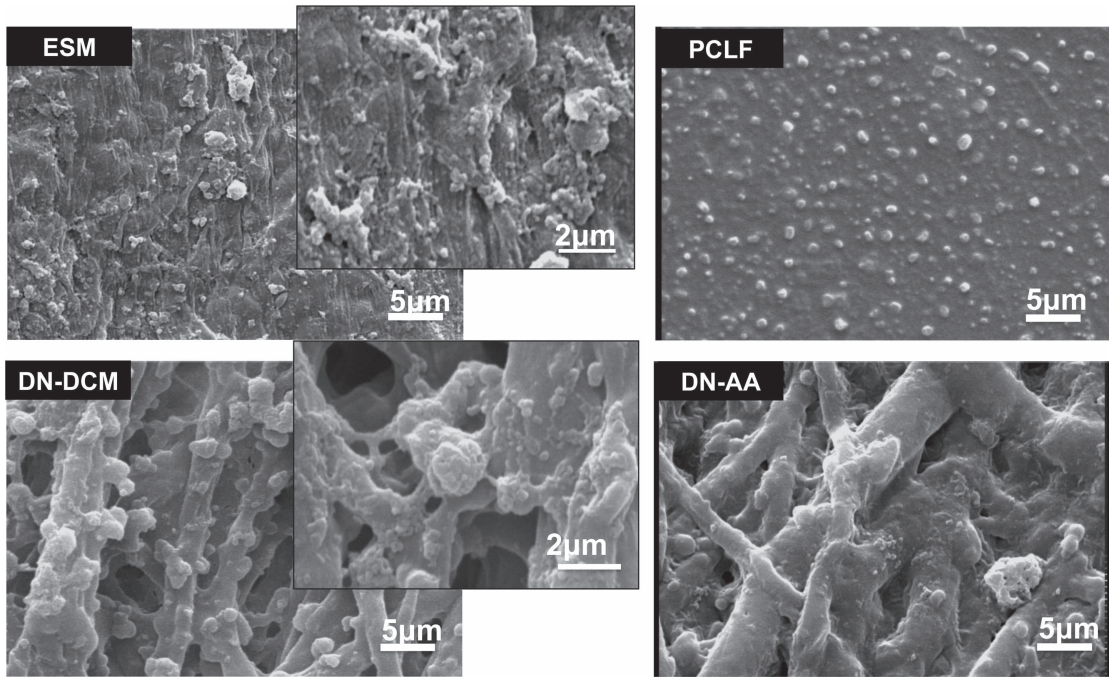

Figure 6. PC12 cell spreading on the various samples; SEM images of PC12 cells after 7 days of culture on ESM, PCLF, DN-DCM and DN-AA scaffolds. Insets are SEM images of the cell seeded scaffolds at higher magnifications.

the biological advantages of ESM giving a versatile biomaterial for tissue-engineered constructs.

4. Conclusions

Herein, we described the fabrication of novel double network fibrous scaffolds consisting of ESM (soft component) and PCLF (hard component) through the one-step, easy and rapid vacuum infiltration approach. This double network fibrous scaffold overcame the weak mechanical properties of ESM and made it suitable for tissue engineering applications. Moreover, depending on the PCLF solvent, it could be possible to change the amount of incorporated PCLF component leading to modulate the mechanical and physical properties of the scaffolds. We also demonstrated that the double network fibrous scaffold of ESM and PCLF considerably affected PC12 cellular responses. For instance, the proliferation of PC12 cells seeded on the ESM:PCLF double network scaffolds prepared with acetic acid solvent significantly enhanced (2.6 times) compared to PCLF film. In summary, double network fibrous scaffold of ESM: PCLF with tunable mechanical and biological properties would potentially be an appropriate promising candidate for the regeneration of nerve tissue.

References

Baláž M 2014 Eggshell membrane biomaterial as a platform for applications in materials science *Acta Biomater.* **10** 3827–43

Colthup N 2012 *Introduction to Infrared and Raman Spectroscopy* (Amsterdam: Elsevier)

Davis G E, Engvall E, Varon S and Manthorpe M 1987 Human amnion membrane as a substratum for cultured peripheral and central nervous system neurons *Dev. Brain Res.* **33** 1–10

Discher D E, Janmey P and Wang Y L 2005 Tissue cells feel and respond to the stiffness of their substrate *Science* **310** 1139–43

Dong Q, Su H, Zhang D, Cao W and Wang N 2007 Biogenic synthesis of tubular SnO_2 with hierarchical intertextures by an aqueous technique involving glycoprotein *Langmuir* **23** 8108–13

Frampton J P, Hynd M R, Shuler M L and Shain W 2011 Fabrication and optimization of alginate hydrogel constructs for use in 3D neural cell culture *Biomed. Mater.* **6** 015002

Golafshan N, Kharaziha M and Fathi M 2016 Tough and conductive hybrid graphene-PVA: alginate fibrous scaffolds for engineering neural construct *Carbon* **111** 752–63

Gong J P 2010 Why are double network hydrogels so tough? *Soft Matter.* **6** 2583

Gong J P, Katsuyama Y, Kurokawa T and Osada Y 2003 Double-network hydrogels with extremely high mechanical strength *Adv. Mater.* **15** 1155–8

Griffin J W, Hogan M V, Chhabra A B and Deal D N 2013 Peripheral nerve repair and reconstruction *J. Bone Joint Surg. Am.* **95** 2144–51

Gu X, Ding F and Williams D F 2014 Neural tissue engineering options for peripheral nerve regeneration *Biomaterials* **35** 6143–56

Haque M A, Kurokawa T and Gong J P 2012 Super tough double network hydrogels and their application as biomaterials *Polymer* **53** 1805–22

Jabbari E, Gruetzmacher J, Lu L, Currier B and Yaszemski M. Development of a novel self-crosslinkable poly (caprolactone fumarate) as a biodegradable and injectable scaffold for bone tissue engineering In *Engineering in Medicine and Biology Society, 2003. Proceedings of the 25th Annual International Conference of the IEEE* 2, 1219–22

Jiankang H, Dichen L, Yaxiong L, BO Y, Hanxiang Z, Qin L, Bingheng L and Yi L 2009 Preparation of chitosan–gelatin hybrid scaffolds with well-organized microstructures for hepatic tissue engineering *Acta Biomater.* **5** 453–61

Kharaziha M, Nikkhah M, Shin S R, Annabi N, Masoumi N, Gaharwar A K, Camci-Unal G and Khademhosseini A 2013 PGS:gelatin nanofibrous scaffolds with tunable mechanical and structural properties for engineering cardiac tissues *Biomaterials* **34** 6355–66

Kharaziha M, Shin S R, Nikkhah M, Topkaya S N, Masoumi N, Annabi N, Dokmeci M R and Khademhosseini A 2014 Tough and flexible CNT-polymeric hybrid scaffolds for engineering cardiac constructs *Biomaterials* **35** 7346–54

Kim J I, Hwang T I, Aguilar L E, Park C H and Kim C S 2016 A controlled design of aligned and random nanofibers for 3D Bi-functionalized nerve conduits fabricated via a novel electrospinning set-up *Sci. Rep.* **6** 23761

Kitahara A K, Suzuki Y, Nishimura Y, Suzuki K, Kiyotani T, Takimoto Y, Nakamura T, Shimizu Y and Endo K 1998 Evaluation of collagen nerve guide in facial nerve regeneration *J. Artif. Organs* **1** 22–7

Koh H S, Yong T, Chan C K and Ramakrishna S 2008 Enhancement of neurite outgrowth using nano-structured scaffolds coupled with laminin *Biomaterials* **29** 3574–82

Kong J and Yu S 2007 Fourier transform infrared spectroscopic analysis of protein secondary structures *Acta Biochimica et Biophys. Sin.* **39** 549–59

Lee T, Chang S C and Peng J F 2010 Tris (8-hydroxyquinoline) aluminum (III)(Alq3) nanowires templated from an eggshell membrane *Thin Solid Films* **518** 5488–93

Martín J and Mijangos C 2008 Tailored polymer-based nanofibers and nanotubes by means of different infiltration methods into alumina nanopores *Langmuir* **25** 1181–7

Nakano T, Ikawa N and Ozimek L 2003 Chemical composition of chicken eggshell and shell membranes *Poultry Sci.* **82** 510–4

Nakayama A, Kakugo A, Gong J P, Osada Y, Takai M, Erata T and Kawano S 2004 High mechanical strength double-network hydrogel with bacterial cellulose *Adv. Funct. Mater.* **14** 1124–8

Nectow A R, Marra K G and Kaplan D L 2012 Biomaterials for the development of peripheral nerve guidance conduits *Tissue Eng.* B **18** 40–50

Özgenel G Y 2003 Effects of hyaluronic acid on peripheral nerve scarring and regeneration in rats *Microsurgery* **23** 575–81

Prabhakaran M P, Kai D, Ghasemi-Mobarakeh L and Ramakrishna S 2011 Electrospun biocomposite nanofibrous patch for cardiac tissue engineering *Biomed. Mater.* **6** 055001

Ruff K J, Devore D P, Leu M D and Robinson M A 2009 Eggshell membrane: a possible new natural therapeutic for joint and connective tissue disorders. Results from two open-label human clinical studies *Clin. Interventions Aging* **4** 235

Runge M B, Dadsetan M, Baltrusaitis J, Knight A M, Ruesink T, Lazcano E A, Lu L, Windebank A J and Yaszemski M J 2010 The development of electrically conductive polycaprolactone fumarate–polypyrrole composite materials for nerve regeneration *Biomaterials* **31** 5916–26

Runge M B, Wang H, Spinner R J, Windebank A J and Yaszemski M J 2012 Reformulating polycaprolactone fumarate to eliminate toxic diethylene glycol: effects of polymeric branching and autoclave sterilization on material properties *Acta Biomater.* **8** 133–43

Sah M K and Rath S N 2016 Soluble eggshell membrane: a natural protein to improve the properties of biomaterials used for tissue engineering applications *Mater. Sci. Eng.* C **67** 807–21

Shalumon K T, Anulekha K H, Nair S V, Nair S V, Chennazhi K P and Jayakumar R 2011 Sodium alginate/poly(vinyl alcohol)/nano ZnO composite nanofibers for antibacterial wound dressings *Int. J. Biol. Macromol.* **49** 247–54

Shin H, Olsen B D and Khademhosseini A 2012a The mechanical properties and cytotoxicity of cell-laden double-network hydrogels based on photocrosslinkable gelatin and gellan gum biomacromolecules *Biomaterials* **33** 3143–52

Shin S R, Bae H, Cha J M, Mun J Y, Chen Y-C, Tekin H, Shin H, Farshchi S, Dokmeci M R and Tang S 2012b Carbon nanotube reinforced hybrid microgels as scaffold materials for cell encapsulation *ACS Nano* **6** 362–72

Shokrgozar M A, Mottaghitalab F, Mottaghitalab V and Farokhi M 2011 Fabrication of porous chitosan/poly (vinyl alcohol) reinforced single-walled carbon nanotube nanocomposites for neural tissue engineering *J. Biomed. Nanotechnol.* **7** 276–84

Sulong A F, Hassan N H, Hwei N M, Lokanathan Y, Naicker A S, Abdullah S, Yusof M R, Htwe O, Idrus R and Haflah N 2014 Collagen-coated polylactic-glycolic acid (PLGA) seeded with neural-differentiated human mesenchymal stem cells as a potential nerve conduit *Adv. Clin. Exp. Med.* **23** 353–62

Tian L, Prabhakaran M P and Ramakrishna S 2015 Strategies for regeneration of components of nervous system: scaffolds, cells and biomolecules *Regen. Biomater.* **2** 31–45

Tian Q, Zhang L, Liu J, Li N, Ma Q, Zhou J and Sun Y 2015 Coaxial electrospun poly(lactic acid)/silk fibroin nanofibers incorporated with nerve growth factor support the differentiation of neuronal stem cells *RSC Adv.* **5** 49838–48

Vogt U F, Gorbar M, Dimopoulos-Eggenschwiler P, Broenstrup A, Wagner G and Colombo P 2010 Improving the properties of ceramic foams by a vacuum infiltration process *J. Eur. Ceram. Soc.* **30** 3005–11

Wang A, Ao Q, Cao W, Yu M, He Q, Kong L, Zhang L, Gong Y and Zhang X 2006a Porous chitosan tubular scaffolds with knitted outer wall and controllable inner structure for nerve tissue engineering *J. Biomed. Mater. Res.* A **79** 36–46

Wang K K, Nemeth I R, Seckel B R, Chakalis-Haley D P, Swann D A, Kuo J W, Bryan D J and Cetrulo C L 1998 Hyaluronic acid enhances peripheral nerve regeneration *in vivo Microsurgery* **18** 270–5

Wang S, Lu L, Gruetzmacher J A, Currier B L and Yaszemski M J 2006b Synthesis and characterizations of biodegradable and crosslinkable poly(epsilon-caprolactone fumarate), poly (ethylene glycol fumarate), and their amphiphilic copolymer *Biomaterials* **27** 832–41

Wang S, Yaszemski M J, Knight A M, Gruetzmacher J A, Windebank A J and Lu L 2009 Photo-crosslinked poly (ε-caprolactone fumarate) networks for guided peripheral nerve regeneration: material properties and preliminary biological evaluations *Acta Biomater.* **5** 1531–42

Wang X, Wang H and Brown H R 2011 Jellyfish gel and its hybrid hydrogels with high mechanical strength *Soft Matter* **7** 211–9

Woo K M, Chen V J and Ma P X 2003 Nano-fibrous scaffolding architecture selectively enhances protein adsorption contributing to cell attachment *J. Biomed. Mater. Res.* A **67** 531–7

Xie J, Macewan M R, Liu W, Jesuraj N, Li X, Hunter D and Xia Y 2014 Nerve guidance conduits based on double-layered scaffolds of electrospun nanofibers for repairing the peripheral nervous system *ACS Appl. Mater. Interfaces* **6** 9472–80

Yang J-Y, Chuang S-S, Yang W-G and Tsay P-K 2003 Egg membrane as a new biological dressing in split-thickness skin graft donor sites: a preliminary clinical evaluation *Chang Gung Med. J.* **26** 153–9

Yang W, Furukawa H and Gong J P 2008 Highly extensible double-network gels with self-assembling anisotropic structure *Adv. Mater.* **20** 4499–503

Yucel D, Kose G T and Hasirci V 2010 Polyester based nerve guidance conduit design *Biomaterials* **31** 1596–603

Zhang S, Huang Y, Yang X, Mei F, Ma Q, Chen G, Ryu S and Deng X 2009 Gelatin nanofibrous membrane fabricated by electrospinning of aqueous gelatin solution for guided tissue regeneration *J. Biomed. Mater. Res.* A **90** 671–9